1-1-2006

Calculation of the cosmogenic nuclide production topographic shielding scaling factor for large areas using DEMs

Alexandru T. Codilean
University of Glasgow, codilean@uow.edu.au

Calculation of the cosmogenic nuclide production topographic shielding scaling factor for large areas using DEMs

Abstract

The recent surge of applications using terrestrial cosmogenic nuclides (TCNs) to calculate catchment-averaged erosion rates from isotopic concentrations in fluvial sediment, and the prospect of coupling TCN production functions with numerical surface process models (SPMs), necessitate a fast and accurate algorithm for the calculation of topographic shielding. Topographic shielding refers to the proportion of the incoming cosmic radiation that is shielded by the surrounding topography, the scaling factor being defined as the ratio of the unshielded (total minus shielded) to the total (or maximum) cosmic ray flux (i.e. the flux received by a horizontal, unobstructed surface). Topography contributes to the reduction of TCN production by obstructing a certain proportion of the incoming flux and by modifying the angle of incidence. Available algorithms calculate the proportion of obstructed radiation by dividing the horizon as seen by the sample (a grid cell in the case of a DEM), into arc segments (usually of equal length) for which the average obstruction heights expressed as zenith angles are calculated. The use of these methods is feasible only when dealing with a small number of isolated samples, since the identification of obstructions when dealing with an entire area is computationally very intensive. This paper describes a method that uses a relief shadow modelling technique to identify those areas of a DEM that are under shadow (i.e. shielded), and thus to account for the obstructed radiation. This method produces results that are very similar to those obtained using a direct implementation of available methods (maximum difference between results of c. 0·1). The method based on relief shadow modelling is also faster than a direct implementation of any available method and can be readily implemented in any GIS system with raster capabilities.

Keywords

Cosmogenic nuclides, scaling factors, topographic shielding, digital elevation models, surface process models, GeoQuest

Disciplines

Medicine and Health Sciences | Social and Behavioral Sciences

Publication Details

Codilean, A. T. (2006). Calculation of the cosmogenic nuclide production topographic shielding scaling factor for large areas using DEMs. Earth Surface Processes and Landforms, 31 (6), 785-794.

Technical Communication

Calculation of the cosmogenic nuclide production topographic shielding scaling factor for large areas using DEMs

Short title: Calculation of topographic shielding using DEMs

Alexandru T. CODILEAN

Department of Geographical and Earth Sciences
University of Glasgow, Glasgow, G12 8QQ, UK
Telephone: +44 (0) 141 330 4782, Fax: +44 (0) 141 330 4894
E-mail: tcodilean@ges.gla.ac.uk

Abstract

The recent surge of applications using terrestrial cosmogenic nuclides (TCNs) to calculate catchment-averaged erosion rates from isotopic concentrations in fluvial sediment, and the prospect of coupling TCN production functions with numerical surface process models (SPMs), both necessitate a fast and accurate algorithm for the calculation of topographic shielding. Topographic shielding refers to the proportion of the incoming cosmic radiation that is shielded by the surrounding topography, the scaling factor being defined as the ratio of the unshielded (total minus shielded) to the total (or maximum) cosmic ray flux (i.e. the flux received by a horizontal, unobstructed surface). Topography contributes to the reduction of TCN production by obstructing a certain proportion of the incoming flux and by modifying the angle of incidence. Available algorithms calculate the proportion of obstructed radiation by dividing the horizon as seen by the sample (a grid cell in the case of a DEM), into arc segments (usually of equal length) for which the average obstruction heights expressed as zenith angles are calculated. The use of these methods is feasible only when dealing with a small number of isolated samples, since the identification of obstructions when dealing with an entire area is computationally very intensive. This paper describes a method that uses a relief shadow modelling technique to identify those areas of a DEM that are under shadow (i.e. shielded), and thus to account for the obstructed radiation. This method produces results that are very similar to those obtained using a direct implementation of available methods (maximum difference between results of ≈ 0.1). The method based on relief shadow modelling is also faster than a direct implementation of any available method and can be readily implemented in any GIS system with raster capabilities.

Keywords: *Cosmogenic nuclides; Scaling factors; Topographic shielding; Digital Elevation Models; Surface Process Models.*

Introduction

Terrestrial cosmogenic nuclides (TCNs) are trace amounts of nuclides produced by the interaction of cosmic rays with the surface of the Earth. Several of these nuclides, including ^{3}He, ^{10}Be, ^{21}Ne, ^{26}Al and ^{36}Cl, are now routinely being measured and have been used in geomorphological studies for the last two decades (e.g., Bierman, 1994; Cockburn and Summerfield, 2004). Initial applications of TCNs focused on measuring *in situ* cosmogenic nuclide concentrations (CICs) in order to provide exposure ages of bedrock surfaces and/or erosion rates. Measurements of CICs in sediments that are leaving a river catchment are now being used to provide time- and space-averaged catchment erosion rates over hundreds to tens of thousands of years (with the timescale depending on the half-life of the nuclide) (e.g., Bierman and Steig, 1996; Granger *et al.*, 1996; Clapp *et al.*, 2000, 2001; Schaller *et al.*, 2001). TCNs are produced mainly by secondary cosmic ray neutron (spallation) and muon bombardment of target elements, such as O and Si, in surficial rocks and sediments. The rapid attenuation of cosmic radiation with depth (approximately 95% is absorbed within the upper 1.8m; Lal, 1991) confines the production of TCNs to the upper few metres of the crust, the production rate decreasing roughly exponentially with depth. The flux of cosmic radiation increases with latitude for latitudes between 0° and 60°, and remains invariant for latitudes $> 60°$; it also increases with a decrease in the thickness of penetrated atmosphere (i.e. with altitude), and therefore the production rate of cosmogenic nuclides at a particular site is mainly a function of geomagnetic latitude and altitude (Lal, 1991; Dunai, 2000; Stone, 2000).

The TCN production rate at a site is also influenced by the site's topographic setting, which can contribute considerably to the reduction of the incoming radiation in areas with an abrupt topography, such as the bottom of a narrow valley or the sides of a nearly vertical cliff. Topography contributes to the reduction of TCN production by (1) shielding a certain proportion of the incoming radiations and (2) modifying the effective attenuation length by changing the angle of incidence on sloping surfaces (Dunne *et al.*, 1999; Gosse and Phillips, 2001). These two effects cannot usually be treated independently, their combination resulting in complicated shielding situations. Identifying obstructions in order to estimate the proportion of shielded cosmic radiation is only feasible when dealing with individual *in situ* bedrock samples, since

this procedure is computationally intensive.

Current applications of TCNs, along with the prospect of coupling TCN production functions with numerical surface process models (SPMs), both necessitate fast and accurate methods for calculating the various scaling factors associated with TCN production calculations. This paper describes a method that uses relief shadow modelling (c.f. Burrough and McDonell, 1998) to calculate the proportion of the incoming cosmic radiation that is shielded by the surrounding topography for large areas using DEMs. The method is computationally less intensive than one that is based on identifying obstructions and is readily implementable in any GIS system with raster capabilities. The method is also suitable for implementation in SPMs.

Shielding by obstructions

The total flux of cosmic radiation (F_{Tot}) received by an object situated on the surface of a flat terrain with an unobstructed view of the sky in all directions is given by (Dunne *et al.*, 1999):

$$F_{Tot} = \int_{\phi=0}^{2\pi} \int_{\theta=0}^{\pi/2} I_0 \sin^m(\theta) \cos(\theta) \mathrm{d}\theta \mathrm{d}\phi \tag{1}$$

where I_0 is the intensity of the incident cosmic radiation, ϕ and θ are the azimuth and elevation angles respectively (θ is measured up from the horizontal; Figure 1A), and m is an experimentally determined constant ($m = 2.3$ is assumed in most studies; Nishiizumi *et al.*, 1989). Integrating with $\theta = 0$ as the lower limit we obtain:

$$F_{Max} = \frac{2\pi I_0}{m+1} \tag{2}$$

where F_{Max} is the maximum cosmic flux received by an object (P) with an unshielded exposure (Figure 1A). For a rectangular obstruction, with height $\sin(\theta_0)$ and width $\sin(\Delta\phi)$ (Figure 1B), the amount of shielded radiation can be calculated by placing the correct limits on the integrals in (1). Doing so yields:

$$F_{Shield} = \frac{\Delta\phi I_0}{m+1} \sin^{m+1}(\theta_0) \tag{3}$$

To account for the obstructed radiation, a topographic shielding factor (C_T) can be calculated as the ratio of the remaining cosmogenic flux ($F_{Max} - F_{Shield}$) to the maximum flux (F_{Max}). For n rectangular obstructions, C_T is given by (Dunne *et al.*, 1999):

$$C_T = 1 - \frac{1}{2\pi} \sum_{i=1}^{n} \Delta\phi_i \sin^{m+1}(\theta_i) \tag{4}$$

Equation (4) is only valid for horizontal target surfaces and is well suited for the calculation of the shielding factor when dealing with only individual *in situ* bedrock samples for which the average azimuth and elevation angles can be directly estimated in the field or calculated from a DEM of the study area (in which case for practical reasons $\Delta\phi = constant$). Using a DEM, the value of C_T at a given cell is obtained by delineating its viewshed and extracting the average elevation angles for every $\Delta\phi$ bin. This procedure requires calculating the position, in spherical polar coordinates, of all the DEM cells relative to the given cell and identifying all those cells that form the horizon (i.e. finding the maximum θ for every ϕ). When calculating C_T for the entire study area and not just for a small number of cells the procedure becomes computationally very intensive. Assuming that the horizon will coincide with the surrounding ridges, a reduction in computing time can be achieved by identifying and eliminating all the non-ridge cells (c.f. O'Callaghan and Mark, 1984; Jenson and Domingue, 1988; Quinn *et al.*, 1991; Freeman, 1991; Tarboton, 1997) and using only the remaining when delineating the viewsheds. In this way the number of cells that need to be queried is reduced but is still high when dealing with large DEMs and complex topographies. Instead of delineating viewsheds, a further simplified and faster approach calculates the spherical polar coordinates for all the surrounding cells, sorts them into $\Delta\phi$ bins, and extracts the maximum elevation angle for each bin, on the assumption that this angle is an accurate estimate of the height of the obstruction. Even though this version is much easier to implement, the assumption it is based on only holds for very small $\Delta\phi$ angles and therefore no real reduction in computing time is achieved.

Relief shadow modeling

Relief shadow modelling or hill shading (Burrough and McDonell, 1998) is a technique that has been widely used in the geosciences to improve the visual qualities of maps depicting three

dimensional information (Horn, 1981; Ding, 1992), for reducing shadow effects in remotely sensed images (Liang *et al.*, 2001), and also in modelling insolation (Kumar *et al.*, 1997). The principle of shadow modelling is based on a model of a three dimensional surface, made of an ideal material, that receives radiation from a point source situated at ∞. The position of this source, relative to the irradiated surface, along with the slope gradient and aspect of each of the DEM cells determines how much radiation each cell receives (Figure 2). A cell that does not receive any radiation from a given source due to its gradient and aspect is said to be in *self-shadow* with respect to that source. Whether a cell receives any radiation is also determined by the configuration of the surrounding topography, as larger features might block the incoming radiation from others. A cell that is blocked from the radiation source by other cells is said to be in *cast-shadow* with respect to that source. Assuming that we are dealing with cosmic radiation, we can calculate the proportion of obstructed radiation by modelling self- and cast-shadows for a range of azimuth (ϕ) and elevation angle (θ) pairs.

Self-shadows

The intensity of the cosmic radiation received from a point source by a terrain element (in our case a DEM cell) depends on the angle of incidence (δ_S) of the radiation, which is a function the azimuth (ϕ_S) and elevation angle (θ_S) of the source, and the slope gradient (β) and aspect (α) of the terrain element (Figure 2). Using the spherical law of cosines, δ_S is given by:

$$\delta_S = \arccos\left[\sin(\theta_S)\cos(\beta) + \cos(\theta_S)\sin(\beta)\cos(\phi_S - \alpha)\right] \tag{5}$$

When $\delta_S > 90^\circ$ the cell does not receive any radiation from that particular source (S), i.e. it is in self-shadow with respect to the source. The calculation of δ is straight forward and is not computationally intensive since there are only three sets of calculations that have to be performed for every DEM cell (i.e. calculating β, α, and δ).

Algorithms for calculating β and α have been given by Horn (1981), Zevenbergen and Thorne (1987), Shanoltz *et al.* (1990), Hickey *et al.* (1994), and Wood (1996) and have also been reviewed by Burrough and McDonell (1998). Implementations of the algorithms for calculating

β and α are also available in virtually any software application dealing with terrain data, and will not be discussed here.

Cast-shadows

Cast-shadows are more difficult to detect than self-shadows, since any objects situated between the radiation source and the terrain element of interest can potentially block the radiation. Cast-shadows can be detected by identifying those cells that are not visible from a given radiation source. If the source is situated at ∞, the radiation path vectors incident on the surface will be parallel for all cells. When $\phi_S \in \{0°, 90°, 180°, 270°\}$ and $\theta_S = 0°$ (i.e. the source is situated either at the north, east, south, or west, and is in the same plane with the x and y coordinates of the DEM cells), cast-shadows can be detected by: (1) identifying all the cells with the same x coordinates (or y, depending on ϕ_S), (2) sorting these cells according to their y (or x) coordinates, in descending or ascending order (again depending on ϕ_S), and (3) detecting whether for a cell with elevation z there are any cells with elevation Z ($Z > z$), situated between itself and the source. All the cells for which the third point is true are blocked from the radiation source and, therefore, are in cast-shadow. For the rest of the cases when $\phi_S \notin \{0°, 90°, 180°, 270°\}$ and $\theta_S \neq 0°$, the coordinate system has to be rotated so that the procedure outlined above can be performed. Such a detection method, based on coordinate rotations, has been proposed by Ding and Sheng (1989), and is outlined here.

For detecting cast-shadows for a radiation source with azimuth ϕ_S and elevation angle θ_S, the x, y, z coordinate system of the DEM has to be rotated so that the radiation source's path vector is in the same plane as x and y and is parallel with either x or y. To achieve this, we first rotate the x, y, z coordinates around the z axis with an angle equal to ϕ_S (Figure 3A). This results in a new coordinate system, x', y', z', where (Ding and Sheng, 1989):

$$\begin{cases} x' = x\sin(\phi_S) + y\cos(\phi_S) \\ y' = y\sin(\phi_S) + x\cos(\phi_S) \\ z' = z \end{cases} \tag{6}$$

We then rotate the x', y', z' coordinate system around the x' axis with an angle equal to θ_S,

and obtain the x'', y'', z'' coordinate system (Figure 3B), where (Ding and Sheng, 1989):

$$\begin{cases} x'' = x' \\ y'' = y' \cos(\theta_S) + z' \sin(\theta_S) \\ z'' = z' \cos(\theta_S) + y' \sin(\theta_S) \end{cases} \tag{7}$$

Combining (6) with (7) we obtain:

$$z'' = z \cos(\theta_S) + [x \cos(\phi_S) - y \sin(\phi_S)] \sin(\theta_S) \tag{8}$$

Every DEM cell $P_{(x_i'', y_i'', z_i'')}$ for which there is another cell $P_{(x_j'', y_j'', Z_j'')}$ located between itself and the radiation source, so that $z_i'' < Z_j''$, is in cast shadow.

Shielding Factor

For a given azimuth (ϕ_S) and elevation angle (θ_S) we can identify all the DEM cells that are in shadow and assign them a weight equal to $\sin^{m+1}(\theta_S)$ (see above). The procedure can be repeated for a range of azimuth and elevation angle pairs, and a shielding factor is obtained from:

$$C_T' = 1 - \frac{\sum_{S=1}^{w} W_S}{\sum_{S=1}^{p(\phi,\theta)} W_S} \tag{9}$$

where, $\sum_{S=1}^{w} W_S$ is the sum of the weights associated with every DEM cell, and $\sum_{S=1}^{p(\phi,\theta)} W_S$ is the sum of the weights associated with the azimuth and elevation angle pairs. When the two sums in (9) are equal, the cell does not receive radiation from any of the (ϕ, θ) pairs, and $C_T' = 0$. When the numerator of (9) is zero, the cell is not shadowed from any of the (ϕ, θ) pairs, and $C_T' = 1$. Equation (9), just like (4), only holds for horizontal target surfaces since it does not account for the effects of slope angle on the effective attenuation length.

Comparison of methods

A high resolution DEM of the Rio Torrente catchment (Sierra Nevada, S. Spain)(Figure 4) has been used to assess the performance of the two methods described above, by calculating

the TCN production topographic shielding scaling factor using both equations (4) and (9). For simplicity we ignore the effects of slope angle on attenuation length when calculating the shielding factors. Although this effect cannot be treated independently, one can argue that the results of both methods would be influenced in the same way should the effect of slope angle on attenuation length be considered and, therefore, by ignoring it we are not introducing bias in the comparison. The Rio Torrente catchment is characterised by the presence of an upstream propagating knickzone that separates two geomorphologically distinct regions: an upper, low relief, high elevation region, and a lower, high relief, low elevation region. The rejuvenated sector of the Rio Torrente is characterised by a narrow and deep valley with very steep surrounding hillslopes dominated by rock and debris slides. This topographic configuration results in high topographic shielding that makes the area suitable for testing and comparing the two methods.

To minimize the effects of averaging, equation (4) has been evaluated using a relatively small bin ($\Delta\phi = 1°$) and the resulting values for C_T are shown in Figure 5A. The method based on relief shadow modelling has been evaluated using pairs of (ϕ, θ) with both ϕ and θ being equal to 5° and the resulting C'_T values are shown in Figure 5B. The difference between the two maps is shown in Figure 5C. With a maximum difference of ≈ 0.1, the two methods produce very similar results, and since both are estimates of a 'true' value that is unknown, it is very difficult to tell which performs better. The differences shown by Figure 5C can be explained in that the method based on equation (4) estimates average obstruction heights only, whereas the method based on shadow modelling takes into account every single cell and thus is more sensitive to the minor changes in landscape characteristics. Furthermore, the number of cells that are averaged to yield the azimuth angle in equation (4) is not only a function of $\Delta\phi$ but also of the distance at which the the obstruction is located from the target cell since the range of cells encompassed by a given $\Delta\phi$ increases with distance (Figure 4). Therefore, even with a small $\Delta\phi$ there is a possibility of under- or overestimating the size of the obstructions. The number of computations involved in identifying obstructions is much higher than for modelling shadows and, therefore, the cumulative effect of roundoff errors is also much higher for C_T than it is for C'_T. In terms of the values obtained ,however, the differences between the two methods are negligible, and it can be argued that the technique based on relief shadow

modelling is less prone to introducing bias in the results. In terms of computing time the calculation of C_T necessitated ≈ 46 hours for $\Delta\phi = 1^\circ$ (and ≈ 5 hours for $\Delta\phi = 5^\circ$) using a P4 class Intel processor whereas C'_T took only ≈ 15 minutes for $\Delta\phi = 5^\circ$ and $\Delta\theta = 5^\circ$.

Concluding remarks

As shown by Figure 5C the two methods produce very similar results, with differences being almost negligible. However, the method based on relief shadow modelling is less prone to under- or overestimating the proportion of obstructed radiation, given that (1) no averaging occurs, and the extent of shadows is calculated taking into account every single DEM cell and (2) the relief shadow modelling approach does not treat the target surface as horizontal, but also takes into account its slope angle and orientation. This method is also computationally less intensive than a method based solely on identifying obstructions and it is readily implementable in any GIS system that has raster capabilities. This aspect is very practical since most often the DEM data used in TCN-related applications are already in a format native to these GIS systems and, therefore, no additional work is needed to transfer the data into new packages. Figure 6 shows that the shadow modelling technique produces very similar results even with a lower number of (ϕ, θ) pairs. It is, therefore, also suitable for implementation in numerical surface process models where the efficiency and speed of the algorithms are important factors.

Acknowledgements

Funding to the author from a Glasgow University Scholarship and a Universities UK - ORS Award are acknowledged. Liam Reinhardt is thanked for providing the source data for the Rio Torrente DEM. Paul Bishop and Trevor Hoey provided comments on an earlier version of the manuscript. The manuscript has also benefitted from the comments of Tibor Dunai.

References

Bierman PR. 1994. Using in situ produced cosmogenic isotopes to estimate rates of landscape evolution: A review from the geomorphic perspective. *Journal of Geophysical Research* **99**(B7): 13885–13896.

Bierman PR, Steig E. 1996. Estimating rates of denudation and sediment transport using cosmogenic isotope abundances in sediment. *Earth Surface Processes and Landforms* **21**: 125–139.

Burrough PA, McDonell RA. 1998. *Principles of Geographic Information Systems*. Oxford University Press.

Clapp EM, Bierman PR, Nichols KK, Pavich M, Caffee M. 2001. Rates of sediment supply to arroyos from upland erosion determined using in situ produced cosmogenic ^{10}Be and ^{26}Al. *Quaternary Research* **55**(2): 235–245.

Clapp EM, Bierman PR, Schick AP, Lekach J, Enzel Y, Caffee M. 2000. Sediment yield exceeds sediment production in arid region drainage basins. *Geology* **28**: 995–998.

Cockburn HAP, Summerfield MA. 2004. Geomorphological applications of cosmogenic isotope analysis. *Progress in Physical Geography* **28**(1): 1–42.

Ding Y. 1992. An improved method for shadow modelling based on Digital Elevation Models. *Proceedings of the GIS/LIS'92 Annual Conference and Exposition* **1**: 178–187.

Ding Y, Sheng Y. 1989. A new method for topographic shadows removal in TM image of mountainous area. *Remote Sensing Application (China)* **2**(1): 9–18.

Dunai TJ. 2000. Scaling factors for production rates of in situ produced cosmogenic nuclides: a critical reevaluation. *Earth and Planetary Science Letters* **176**: 157–169.

Dunne J, Elmore D, Muzikar P. 1999. Scaling factors for the rates of production of cosmogenic nuclides for geometric shielding and attenuation at depth on sloped surfaces. *Geomorphology* **27**: 3–11.

Freeman TG. 1991. Calculating catchment area with divergent flow based on a regular grid. *Computers in Geosciences* **17**: 413–422.

Gosse JC, Phillips FM. 2001. Terrestrial in situ cosmogenic nuclides: theory and application. *Quaternary Science Reviews* **20**: 1475–1560.

Granger DE, Kirchner JW, Finkel RC. 1996. Spatially averaged long-term erosion rates measured from in situ-produced cosmogenic nuclides in alluvial sediment. *The Journal of Geology* **104**: 249–257.

Hickey R, Smith A, Jankowski P. 1994. Slope length calculations from a DEM within Arc/Info GRID. *Computing, Environment and Urban Systems* **18**(5): 365–380.

Horn BKP. 1981. Hill shading and the reflectance map. *Proceedings of the IEEE* **69**(1): 14–47.

Jenson SK, Domingue JO. 1988. Extracting topographic structure from digital elevation data for geographic information system analysis. *Photogrammetric Engineering and Remote Sensing* **54**(1): 593–600.

Kumar L, Skidmore AK, Knowles E. 1997. Modelling topographic variation in solar radiation in a GIS environment. *International Journal for Geographical Information Science* **11**(5): 475–497.

Lal D. 1991. Cosmic ray labeling of erosion surfaces - In situ nuclide production rates and erosion models. *Earth and Planetary Science Letters* **104**: 424–439.

Liang S, Fang H, Chen M. 2001. Atmospheric correction of Landsat ETM+ land surface imagery: I. Methods. *IEEE Transactions on Geosciences and Remote Sensing* **39**(11): 2490–2498.

Nishiizumi K, Winterer EL, Kohl CP, Lal D, Arnold JR, Klein J, Middleton R. 1989. Cosmic ray production rates of ^{10}Be and ^{26}Al in quartz from glacially polished rocks. *Journal of Geophysical Research* **94**(B12): 17907–17015.

O'Callaghan JF, Mark DM. 1984. The extraction of drainage networks from digital elevation data. *Computer Vision, Graphics and Image Processing* **28**: 328–344.

Quinn P, Beven K, Chevallier P, Planchon O. 1991. The prediction of hillslope flow paths for distributed hydrological modelling using digital terrain models. *Hydrological Processes* **5**: 59–80.

Schaller M, von Blanckenburg F, Hovius N, Kubik PW. 2001. Large-scale erosion rates from in situ-produced cosmogenic nuclides in european river sediments. *Earth and Planetary Science Letters* **188**: 441–458.

Shanoltz VO, Desai CJ, Zhang N, Kleene JW, Metz CD. 1990. Hydrological/Water quality modeling in a GIS environment. ASAE Paper 90-3033, St Joseph, MI: ASAE.

Stone JO. 2000. Air pressure and cosmogenic isotope production. *Journal of Geophysical Research* **105**(14): 23753–23760.

Tarboton DG. 1997. A new method for the determination of flow directions and upslope areas in grid digital elevation models. *Water Resources Research* **33**: 309–319.

Wood JW. 1996. *The geomorphological characterisation of digital elevation models*. Ph.D. Dissertation, Department of Geography, University of Leicester, Leicester, U.K.

Zevenbergen LW, Thorne CR. 1987. Quantitative analysis of land surface topography. *Earth Surface Processes and Landforms* **12**: 12–56.

Figure captions

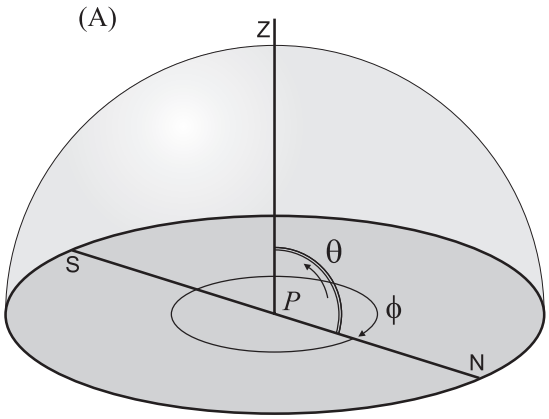

$$F_{Received} = F_{Max}$$

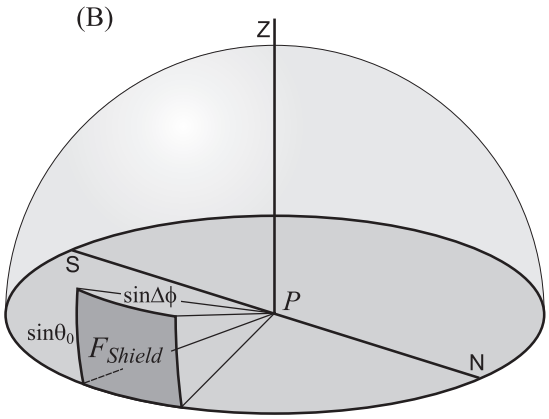

$$F_{Received} = F_{Max} - F_{Shield}$$

Figure 1.

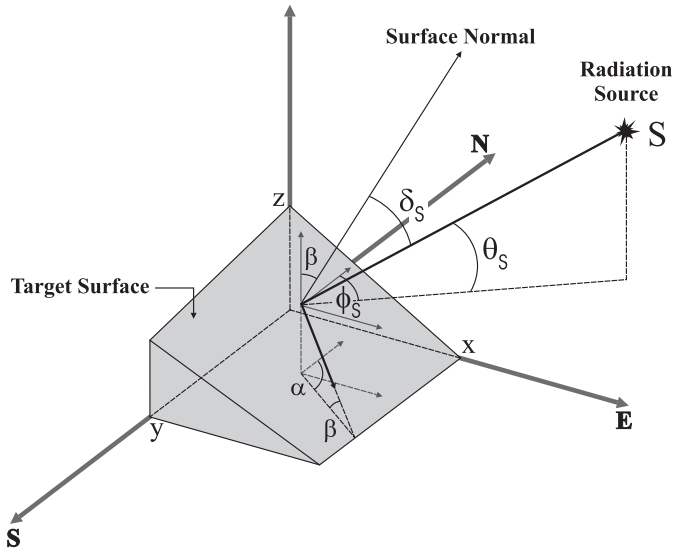
Surface Normal
Radiation
Source
S
N
z
δ_S
θ_S
β
Target Surface
ϕ_S
x
α
β
y
E
S

Figure 2.

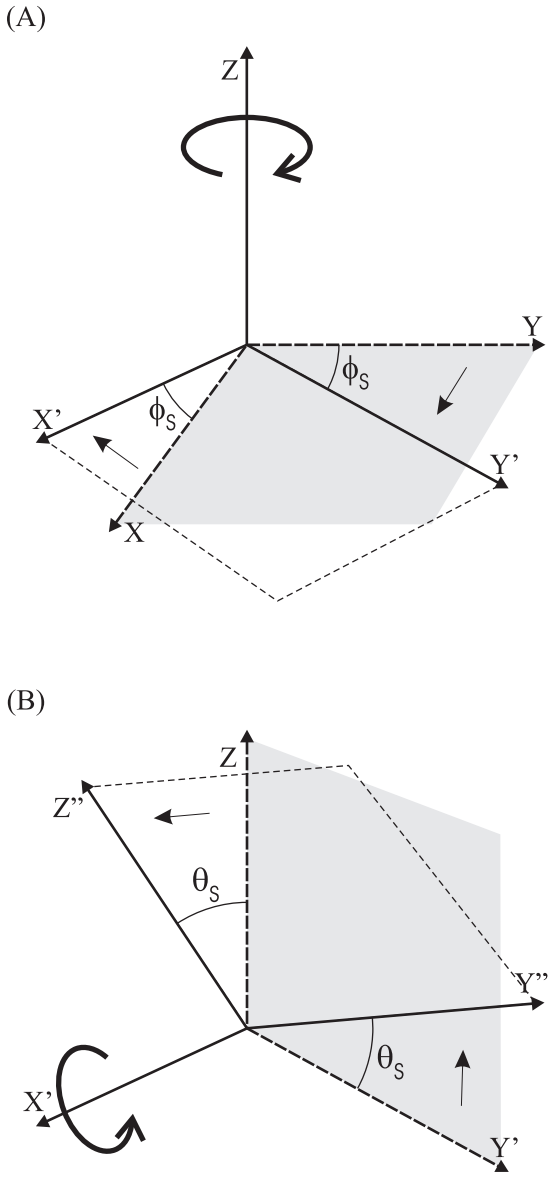

Figure 3.

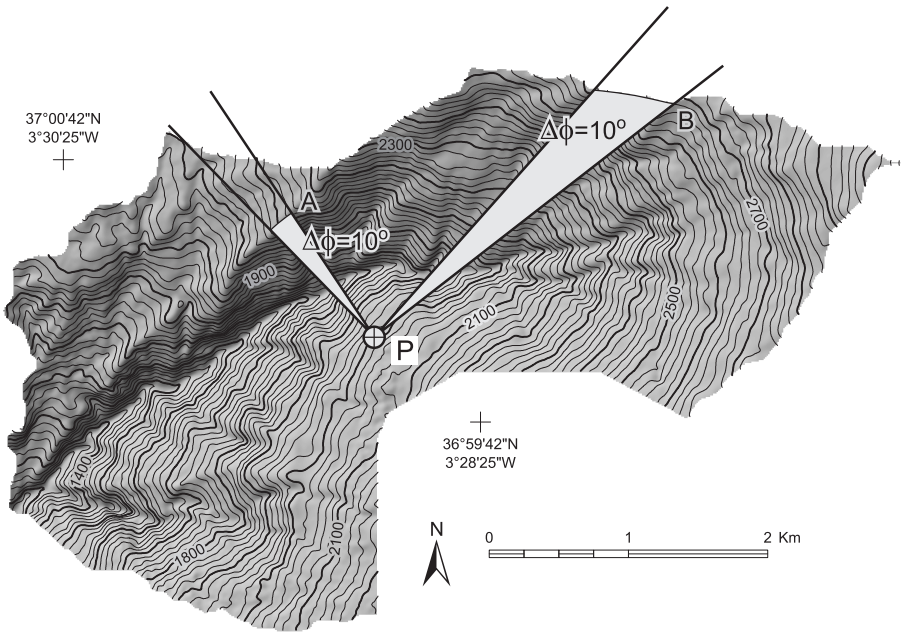
37°00'42"N
3°30'25"W
A
Δϕ=10°
B
Δϕ=10°
P
2300
1900
2100
2700
2500
1400
1800
2100
36°59'42"N
3°28'25"W
N
0
1
2 Km

Figure 4.

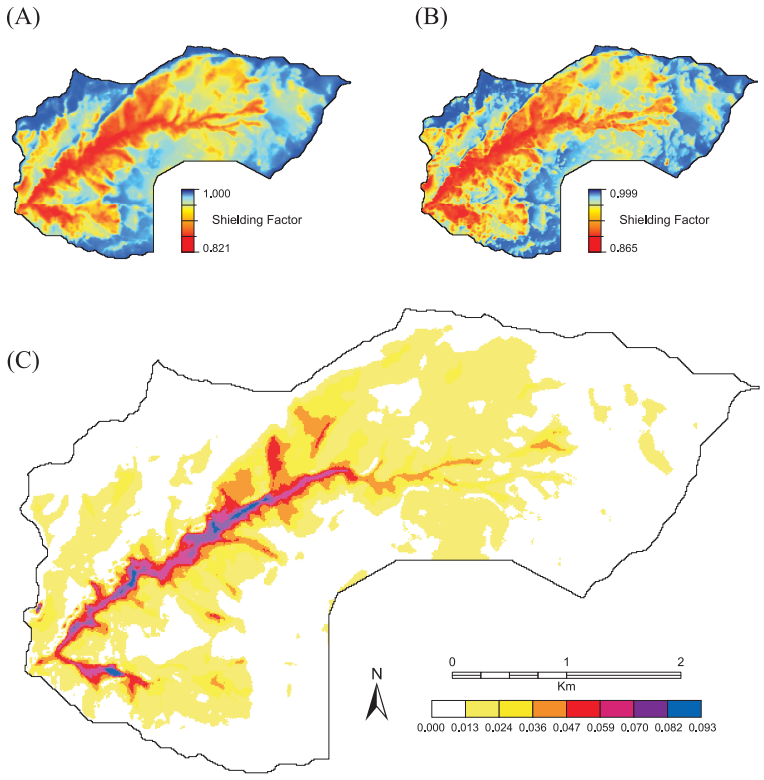
(A)
1.000
Shielding Factor
0.821
(B)
0.999
Shielding Factor
0.865
(C)
N
0
1
2
Km
0.000 0.013 0.024 0.036 0.047 0.059 0.070 0.082 0.093

Figure 5.

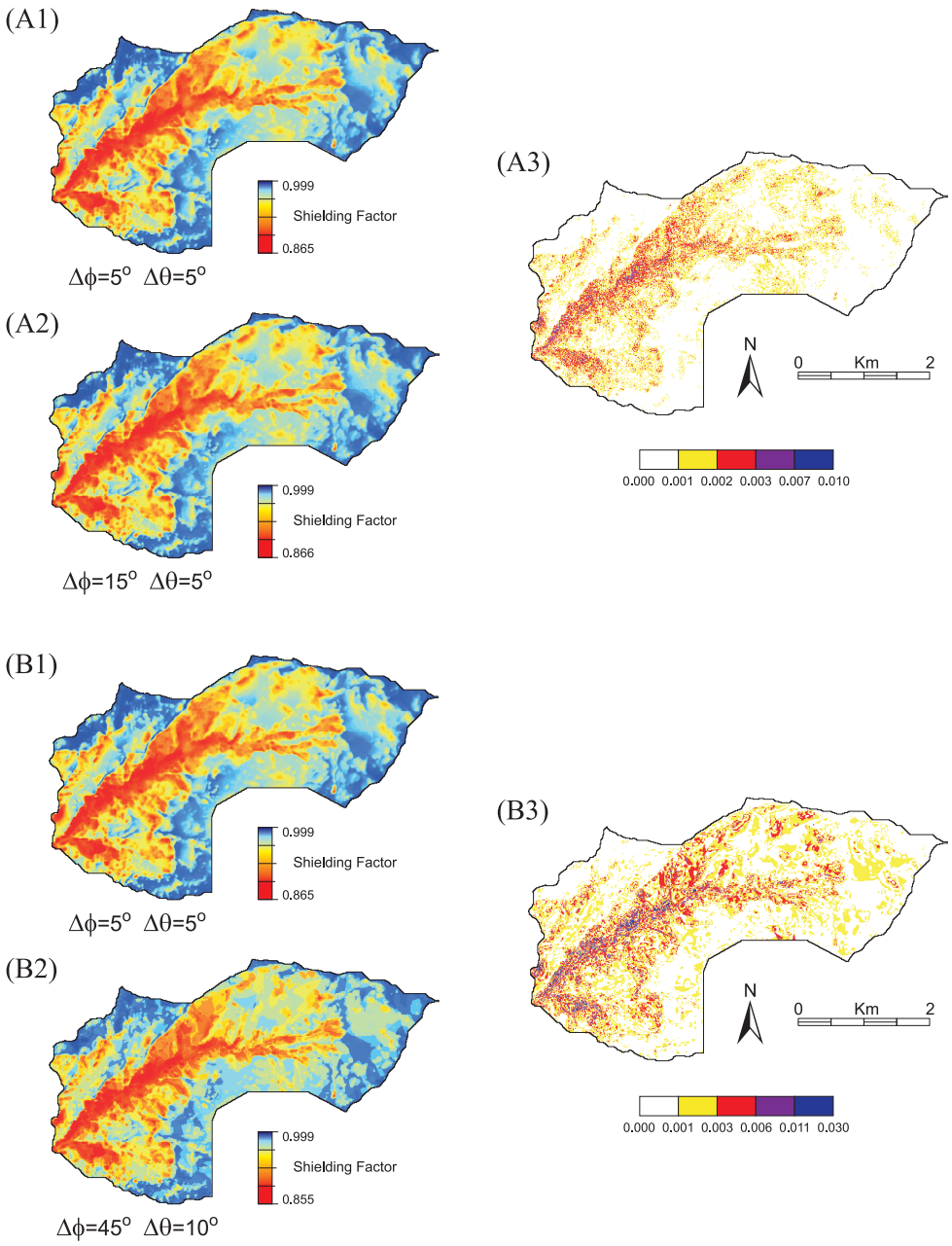
(A1)
0.999
Shielding Factor
0.865
Δϕ=5° Δθ=5°
(A2)
0.999
Shielding Factor
0.866
Δϕ=15° Δθ=5°
(A3)
N
0 Km 2
0.000 0.001 0.002 0.003 0.007 0.010
(B1)
0.999
Shielding Factor
0.865
Δϕ=5° Δθ=5°
(B2)
0.999
Shielding Factor
0.855
Δϕ=45° Δθ=10°
(B3)
N
0 Km 2
0.000 0.001 0.003 0.006 0.011 0.030

Figure 6.